International Journal of Multidisciplinary Research and Publications
ISSN (Online): 2581-6187

Exploring the Optoelectronic Potential of Cubic Halide-Perovskite KFeX3 (X = Cl, Br): A DFT Perspective

Ahmed Shahzad[1], Naseeb Ahmad[2], Muhammad Arbaz[3*], Ifra Shahzadi[4], Moazama Ahsan[1], Zia Ur Rehman[5], Rizwan Akbar[6], Muhammad Kashif Bashir[7], Shahbaz Ali[4*]

[1]Institute of Physics, Khwaja Fareed University of Engineering and Information Technology, Rahim Yar Khan-64200, Pakistan
[2]Department of Physics, Baba Guru Nanak University, Nankana Sahib-39100, Pakistan
[3]Department of Chemistry, Institute of Chemical Sciences, Government College University Lahore, 5400, Pakistan
[4]Institute of Chemistry, Khwaja Fareed University of Engineering and Information Technology, Rahim Yar Khan-64200, Pakistan
[5]School of Energy & Power Engineering, Xi'an Jiaotong University Xi'an, Shaanxi 710049 China
[6]Department of Chemistry, COMSATS University Islamabad, Lahore, Pakistan
[7]Institute of Physics, The Islamia university of Bahawalpur, 63100, Pakistan
Email address: Kashifkarim68@gmail.com

Abstract*—The present work deals with exploring the electronic, optical, and structural properties of cubic halide-perovskites KFeX3 (X= Cl, Br) through first-principles calculations. The study used the CASTEP code with the PBE exchange-correlation functional in the GGA framework. Ultra-soft pseudo-potential (USP) plane-wave. DFT calculations were carried out for this study. The calculated elastic constants of KFeCl3 and KFeBr3 in their cubic phases supported their mechanical stability. Applying Pugh´s criteria, it is clear that neither of the materials is classified as a brittle material. Electronic band structure analysis indicates that KFeCl3 has an indirect band gap and KFeBr3 possesses a direct band gap, which is consistent with previous reports. Moreover, partial density of states (PDOS) and total density of states (TDOS) were also employed to analyze the electron localization of various bands. Peaks were fitted to the dispersion relation of a hypothetical dielectric function to determine the optical transitions within these compounds. These materials are insulating at 0 K and semiconductors above 0 K rather like the normal BCS metals. The real part of the dielectric function is rather flat with the energy, while the imaginary part of the dielectric function displays a broad spectral width with the energy, which achieves the overall transparency of the inevitable UV-active optoelectronic devices*.

***Keywords*—** *KFeCl3; Density Functional Theory; PDOS; KFeBr3; CASTEP*.

I. INTRODUCTION

To date, perovskite materials have quickly become one of the most exciting materials for research in the field of solar cell technology due to their versatility in properties that could allow them to increase the efficiency of these devices [1]. These materials have optoelectronic properties such as tunable energy band gap, wide absorption band, and a common point defect [2]. Moreover, owing to the large charge diffusion lengths, low carrier effective masses, high-power conversion efficiency (PCE), and high charge carrier mobility of perovskites. Solar energy is the most abundant, cost-effective, and sustainable power source, although the current harnessing of solar energy via traditional photovoltaic technologies remains expensive compared to fossil fuel alternatives.

Halide perovskites (ABX_3), where A is a cation, B is a Pb^{2+}, Sn^{2+}, etc., and X is halide have attracted worldwide attention from many different scientific disciplines due to their abundance in nature and high performance [3]. Those materials offer a great range of properties and can be formed into thin films, as well as a variety of smaller structures, such as quantum dots, nanocrystals, nanowires, nanorods, nanoparticles as well as some macroscopic crystals. This makes them very appealing for a variety of different uses. Therefore, the question of whether perovskite cells would ever exceed the traditional silicone-based technology of the decades to come is forefront of everybody's lips [4].

Halide perovskites frequently exhibit temperature-induced structural phase transitions, with different crystallographic phases present in various thermal states including cubic, tetragonal, and orthorhombic forms [5]. Among them, the high-temperature phase is the cubic phase and it is preferred more at high temperatures than other phases. Although perovskites were known long ago, the popularity of perovskites increased substantially after the introduction of perovskite solar cells in 2009 [6]. A widespread surge in halide perovskites occurred in the demand (since 2009) due to the high PCE stability of all photovoltaic cells from 3.8% to 25.2% by 2019.

Despite significant strides in research, challenges persist in harnessing halide perovskites for widespread commercial use [7]. These challenges necessitate innovative solutions to address issues such as cost-effectiveness, efficiency, and long-term stability. The current leading halide perovskites, notably those based on methylammonium lead trihalide ($MAPbX_3$, where X can be Cl, Br, or I), incorporate organic components vulnerable to degradation upon exposure to environmental factors like air or moisture, thus compromising their stability [8]. Moreover, the presence of lead in these hybrid perovskites raises environmental concerns, further highlighting the

Ahmed Shahzad, Naseeb Ahmad, Muhammad Arbaz, Ifra Shahzadi, Moazama Ahsan, Zia Ur Rehman, Rizwan Akbar, Muhammad Kashif Bashir, Shahbaz Ali, "Exploring the Optoelectronic Potential of Cubic Halide-Perovskite KFeX3 (X = Cl, Br): A DFT Perspective," *International Journal of Multidisciplinary Research and Publications (IJMRAP)*, Volume 7, Issue 5, pp. 56-62, 2024.

urgency for the development of lead-free alternatives to propel perovskite-based technologies forward. Furthermore, despite their promise, lead-based hybrid perovskites exhibit a lower dielectric constant compared to silicon, resulting in heightened charge carrier recombination rates that impede photovoltaic performance [9]. Addressing these shortcomings is crucial for optimizing the efficiency and stability of perovskite-based devices.

In consequence, inorganic perovskites have been suggested as an alternative to hybrid perovskites for a variety of devices due to their close crystallography, and physical properties with better stability. Even though a lot of attention has been given to the exploration of Pb-free inorganic metal halide perovskites, the research work on their K-based counterparts is not at the same level [10]. In this study, we delve into the properties of K-based perovskites, specifically $KFeX_3$ (X = Cl, Br), aiming to elucidate their relevance to photovoltaic and optoelectronic applications, with a particular emphasis on the underexplored mechanical and partially explored optical aspects.

Existing literature on $KFeX_3$ (X = Cl, Br) is scarce, particularly regarding their phase transition behavior, stability, and electronic bandgap. Thus, there exists a significant gap in knowledge necessitating further investigation. Through our research, we endeavor to bridge these gaps and shed light on the potential of K-based perovskites for photovoltaic and optoelectronic applications, drawing comparisons with their K-based counterparts.

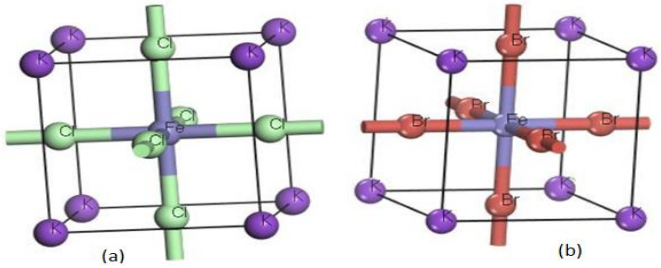

Fig. 1: Crystal Structure for (a) $KFeCl_3$ (b) $KFeBr_3$

II. Methodology and Geometry Optimization Details

Ternary halide-perovskites with cubic structures are studied in this study, with a special focus on $KFeBr_3$ and $KFeCl_3$ compounds. Both of these compounds have the same space group which is Pm3 m. For both compounds, the atomic position for K atoms is consistent at (0.0, 0.0, 0.0) while for Fe atoms it's (0.5, 0.5, 0.5). In the case of Br and Cl atoms positions are (0, 0.5, 0.5) in $KFeBr_3$ and $KFeCl_3$ respectively [11]. The elemental configurations are as follows: K: $1s^2,2s^2,2p^6,3s^2,3p^6,4s^1$; Fe: $1s^2,2s^2,2p^6,3s^2,3p^6,3d^6,4s^2$; Br: $1s^2,2s^2,2p^6,3s^2,3p^6,4s^2,3d^{10},4p^5$; Cl: $1s^2,2s^2,2p^6,3s^2,3p^5$. The CASTEP code is used to analyze structural electronic and optical properties based on Density Functional Theory (DFT) [12]. This method is computationally efficient because it does not require a priori specification of orbital shapes. The inner shell electrons interact with the nuclei to form an ion core that interacts with valence electrons leading to fast convergence of electron-ion potential. To eliminate boundary effects a supercell with dimensions of 8 ×8×8 Å is used for both compounds. Geometry optimization is performed on the supercell followed by computation of desired properties. The total energy per atom is approximately 2×10^{-5} eV residual forces on atoms during geometry optimization 0.05 eV/Å. The Monkhorst Pack grid was employed with a k-mesh of size 1 × 1 × 1, and an energy cutoff of 353.69 eV was used for all calculations over the full Brillouin zone. For calculating elastic constants, the number of steps for each strain is set to 4 with a maximum strain amplitude of 0.002. External stress (GPa) and equivalent hydrostatic pressure are maintained at zero during geometry optimization [13].

TABLE 1: Comparison of lattice constant, cell volume, and band gap of present and previously studied materials.

Co-relational Functional	Lattice Constant (Å)	Cell Volume $(Å)^3$	Band Gap (eV)
$KFeBr_3$	5.19	140.05	1.73
$KFeCl_3$	4.88	116.21	1.64
$NaZnF_3$[14]	4.11	69.26	3.167
$NaSrF_3$ [15]	4.44	87.52	---
$NaGeBr_3$ [16]	5.53	169.39	2.90

III. Results and Discussion

3.1 Structure Analysis

We first optimized the geometries of the designed supercells for both compounds. We utilized the Murnaghan state equation and minimized the total energy of the crystals to find out equilibrium lattice parameters. Many values of lattice constant were tried out and results were computed [17]. Around the equilibrium volume, Total energy vs Unit cell volume was calculated. The band gaps came out to be 0.239 eV for $KFeBr_3$ and 0.138 eV for $KFeCl_3$ after this [18]. By optimizing geometry 'optimized lattice parameters' were found to be equal to 5.1931 Å and 4.880047 Å for $KFeBr_3$ and $KFeCl_3$ respectively which are in good agreement with previously reported data shown in Table I thus confirming the correctness and applicability of our ab initio calculation methods. It should be noted that there is no published work on these compounds in literature so far therefore further measurements will have to be carried out to verify our results accordingly. The relationship of crystals to applied forces is governed by elastic constants, which are useful for understanding the mechanical behavior of solids. In a crystal with cubic symmetry, there are three different elastic constants (C_{11}, C_{12}, and C_{44}) that control its mechanical properties such as rigidity or stability. These values (C_{ij}) were measured and can be found in Table 2 alongside other information like bulk modulus B which can also be determined from them by using this equation:

$$B = (C_{11} + 2C_{22}) / 3 \quad (1a)$$

The requirements for mechanical stability are met if the subsequent elastic constants are satisfied: $C_{11} > 0$, $C_{44} > 0$, $(C_{11}–C_{12}) > 0$, $(C_{11}+2C_{12}) > 0$, and $C_{12}B < C_{11}$. As revealed in Table 2, this is how they relate to each other. A (anisotropy factor), E (Young's modulus), ν (Poisson's ratio), and B/G (Pugh's index to shear modulus ratio) [19].

$$A = (2C_4) / (C_{11} - C_{12}) \quad (2a)$$

Ahmed Shahzad, Naseeb Ahmad, Muhammad Arbaz, Ifra Shahzadi, Moazama Ahsan, Zia Ur Rehman, Rizwan Akbar, Muhammad Kashif Bashir, Shahbaz Ali, "Exploring the Optoelectronic Potential of Cubic Halide-Perovskite KFeX3 (X = Cl, Br): A DFT Perspective," *International Journal of Multidisciplinary Research and Publications (IJMRAP)*, Volume 7, Issue 5, pp. 56-62, 2024.

$$E = (9BG) / (3B + G) \quad (3a)$$
$$v = (3B - 2G) / 2(2B + G) \quad (4a)$$
$$G = (G_R + G_v) / 2 \quad (5a)$$
$$Gv = (C_{11} - C_{12} + 3C_{44}) / 5 \quad (6a)$$
$$G_R = (C_{11} - C_{12})5C_{44} / 3(C11 - C12) + 4C_{44} \quad (7a)$$

TABLE 2: C_{11} C_{22} Young Modulus poisons Ratio of $KFeCl_3$ and $KfeBr_3$

Parameters	$KFeCl_3$	$KFeBr_3$
C11	70.01	56.19
C22	14.28	12.61
C44	19.32	14.54
B	32.86	27.14
A	0.69	0.67
G	22.38	17.11
E	54.72	42.41
N	0.31	0.33
B/G	1.47	1.59

The B/G ratio is a good way to tell how bendy or breakable something [20]. If this number goes less than 1.75, they're calling that material brittle, over 1.75 means it's ductile. According to Pugh's criteria, $KFeCl_3$ and $KFeBr_3$ are both brittle. Another indicator for this is Poisson's ratio (v) which helps decide whether materials are ductile or brittle [21]. If things have a poison ratio above 0.26 then they're said to be able to stretch but if not. Based on this, the materials fall into the category of being fragile ones also. Additionally, the study of the elasticity anisotropy factor (A) in both compounds also gives us some insight into their properties [22]. If it equals 1 then it is isotropic otherwise, when there are deviations from this value it means that there is anisotropy. The analysis shown in Table 2 demonstrates that each compound has different A values which indicates they display different characteristics depending on directionality.

In Table 2, the data shows the Shear Modulus G [GPa], Bulk Modulus B [GPa], Young's Modulus E [GPa], Anisotropy factor A, Poisson's ratio v, Pugh's index ratio B/G at equilibrium volume.

Electronic Properties

An electronic band structure is a description of the energy levels available to electrons in a solid (energy band) and the absence of states where electrons cannot be found (band gap). Important bands are the valence band, which is located below the Fermi level (EF), and the conduction band, which is situated above it. At zero kelvin temperature or absolute zero (0 K), EF coincides with the valence band peak, without taking into account finite temperatures. The energy offset between valence band maximum (VBM) and conduction band minimum (CBM) delimits the forbidden region. In a direct band gap, VBM and CBM are aligned directly on top of each other; while in an indirect bandgap, their alignment is not exact.

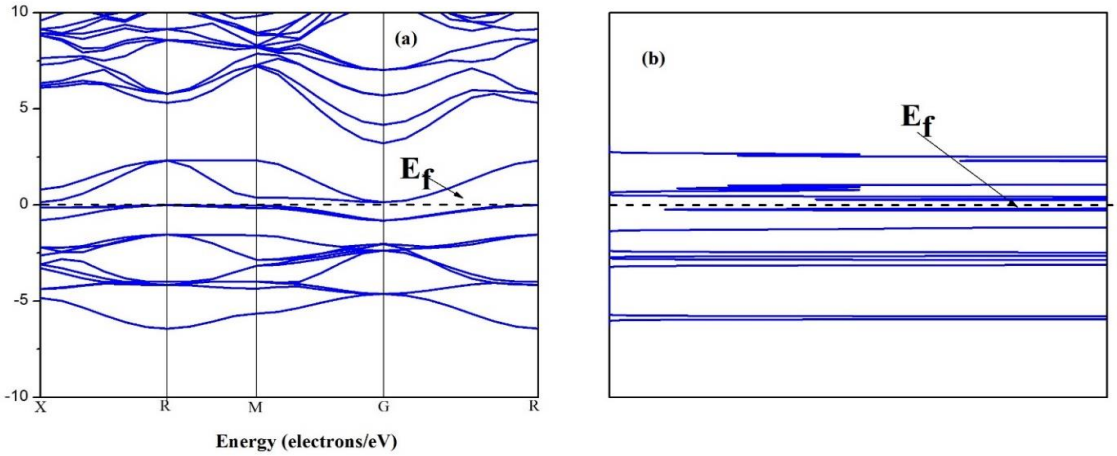

Fig. 2: (a) Band Structure, (b) TDOS of $KFeCl_3$

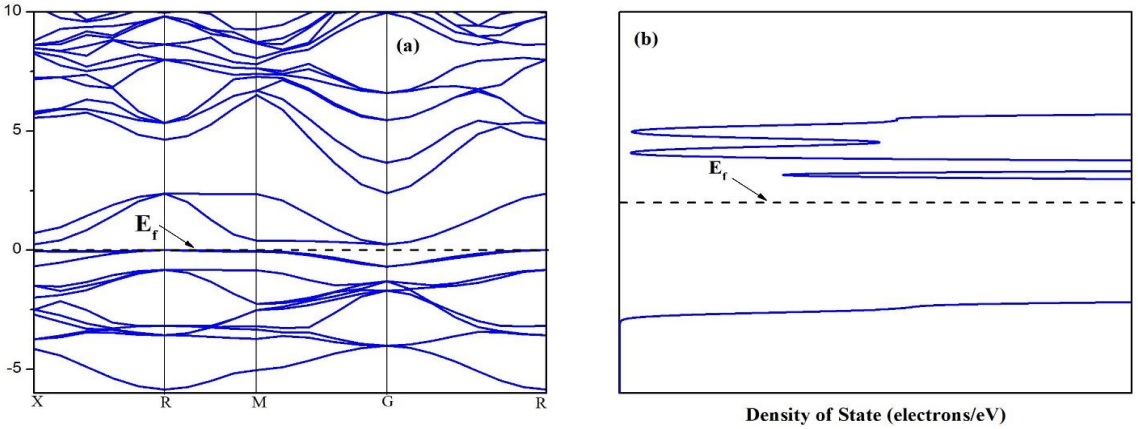

Fig. 3: (a) Band Structure, (b) TDOS of $KFeBr_3$

Ahmed Shahzad, Naseeb Ahmad, Muhammad Arbaz, Ifra Shahzadi, Moazama Ahsan, Zia Ur Rehman, Rizwan Akbar, Muhammad Kashif Bashir, Shahbaz Ali, "Exploring the Optoelectronic Potential of Cubic Halide-Perovskite KFeX3 (X = Cl, Br): A DFT Perspective," *International Journal of Multidisciplinary Research and Publications (IJMRAP)*, Volume 7, Issue 5, pp. 56-62, 2024.

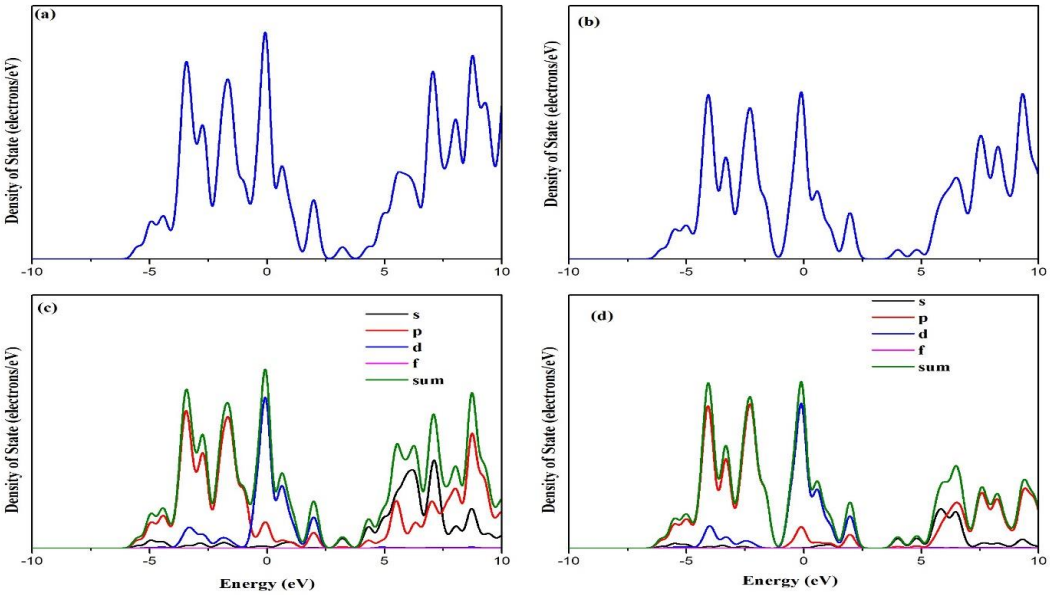

Fig. 2: (a) TDOS of $KFeBr_3$ (b) TDOS of $KFeCl_3$ (c) PDOS of $KFeBr_3$ (d) PDOS of $KFeCl_3$

As shown in Fig. 3(a), there is a direct band gap observed at 1.73eV between the VBM (Valence Band Maximum) and CBM (Conduction Band Minimum) of KFeBr3 during electronic band structure analysis. At absolute zero temperature, this substance acts as an insulator but becomes a semiconductor with an increase in temperature. Unlike this, KFeCl3 has an indirect band gap whose magnitude is 1.64 eV; just like KFeBr3, it shows insulating properties at T = 0K and semiconducting behavior at high temperature.

The band structure is shown in Fig. 2b and 3b together with the density of states (DOS). Because of a lack of experimental data for valence bandwidths and band gaps from literature sources, our results were compared with other theoretical studies as compiled in Table 1. The total density of states (TDOS) for KFeBr3 and KFeCl3 are depicted in Fig. 4a and 4b, respectively. For KFeBr3, TDOS is centered at -0.055964eV while that for KFeCl3 is located at -0.1664eV showing a strong peak and main trough at 9.8432eV for KFeBr3 and 9.2279eV for KFeCl3, respectively. Various orbital contributions such as s, p, d, f, etc. can be identified from partial density of states (PDOS) curves illustrated in Fig. 4c and 4d. Analysis of PDOS reveals primary s peak for KFeBr3 at 7.1360eV and for KFeCl3 at 2.163eV; also observed is main p peak at -1.672eV for KFeBr3 and at-2.2819eV for KFeCl3, while the dominant peak appears at -0.0992 eV for KFeBr3 and -0 .1185 eV for KFeCl3. Fig.5 represents individual elemental PDOSs for potassium (K), iron (Fe), bromine (Br), and chlorine (Cl). It should be noted that each element has its specific features with regard to peak position or intensity which are marked on the graph while all energy values are given relative to Fermi level (E).

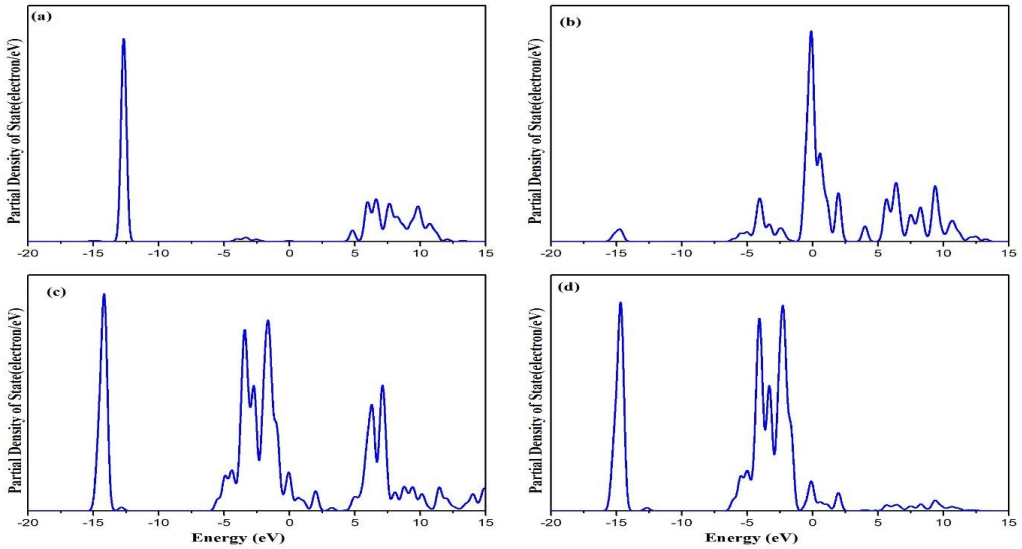

Fig. 3: Elemental PDOS: (a) K-PDOS (b) Fe-PDOS (c) Br-PDOS (d) Cl-PDOS

Ahmed Shahzad, Naseeb Ahmad, Muhammad Arbaz, Ifra Shahzadi, Moazama Ahsan, Zia Ur Rehman, Rizwan Akbar, Muhammad Kashif Bashir, Shahbaz Ali, "Exploring the Optoelectronic Potential of Cubic Halide-Perovskite KFeX3 (X = Cl, Br): A DFT Perspective," *International Journal of Multidisciplinary Research and Publications (IJMRAP)*, Volume 7, Issue 5, pp. 56-62, 2024.

Optical Properties

To understand the reflective properties, absorption coefficients, refractive indices, relative permittivity, and energy-loss functions of $KFeBr_3$ and $KFeCl_3$ were studied. Frequency dependent optoelectric response was taken as the basis for investigating these parameters. The research considered electromagnetic wave (light) interaction with matter being studied. Fig. 6 displays measured values for some optical quantities of $KFeBr_3$ and $KFeCl_3$. The complex dielectric function ε(ω), which relates different optical parameters together, was used to get more information about them in general terms.

$$\varepsilon(\omega) = \varepsilon_1(\omega) + i\varepsilon_1(\omega) \quad (1b)$$

There are two parts of the dielectric equation, which are $\varepsilon_1(\omega)$ and $\varepsilon_2(\omega)$, showing the real and imaginary parts respectively. The actual part is an indicator of material polarization while the unreal part represents energy dissipation i.e., loss function. Some optical quantities such as refractive index (n(ω)), energy loss (L(ω)), absorption coefficient (I(ω)), and reflectivity (R(ω)) were calculated [23] with given formulas. Fig 6 shows the data from $KFeBr_3$ and $KFeCl_3$ compounds together.

$$n(\omega) = \left[\varepsilon_1(\omega)/2 + \{\varepsilon_1^2(\omega) + \varepsilon_1^2(\omega)\}^{\frac{1}{2}}/2\right]^{1/2} \quad (2b)$$

$$I(\omega) = 2^{1/2}\omega[\{\varepsilon_1^2\omega) + \varepsilon_1^2(\omega)\}^{1/2} - \varepsilon_1(\omega)]^{1/2} \quad (3b)$$

$$L(\omega) = -Im(\varepsilon(\omega) - 1) = \varepsilon_2(\omega) / \varepsilon_1(\omega)^2 + \varepsilon_2(\omega)^2 \quad (4b)$$

$$R(\omega) = (n + k - 1) / ((n + k + 1) \quad (5b)$$

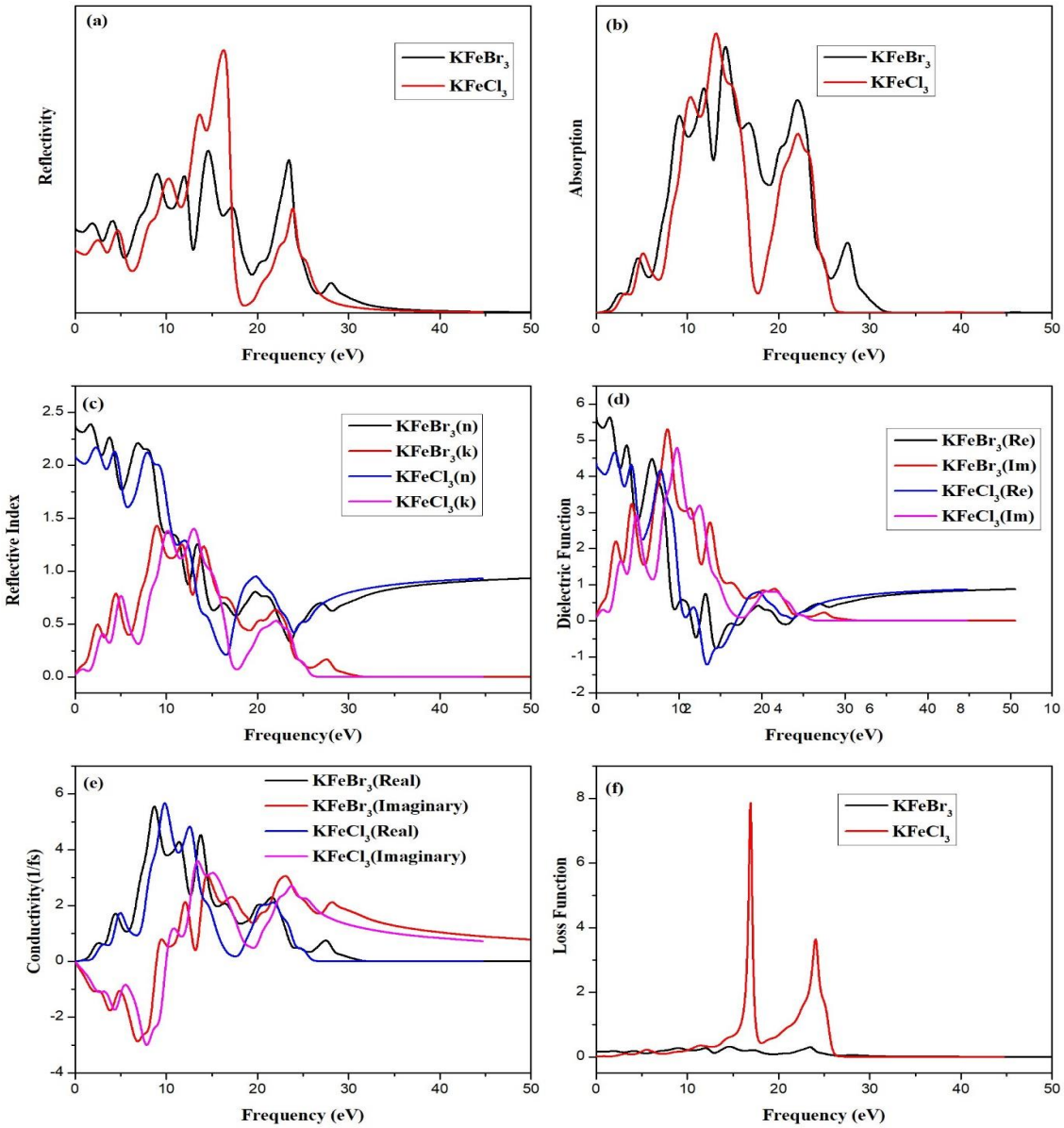

Fig. 4: Optical properties of $KFeBr_3$ and $KFeCl_3$ perovskites

Ahmed Shahzad, Naseeb Ahmad, Muhammad Arbaz, Ifra Shahzadi, Moazama Ahsan, Zia Ur Rehman, Rizwan Akbar, Muhammad Kashif Bashir, Shahbaz Ali, "Exploring the Optoelectronic Potential of Cubic Halide-Perovskite KFeX3 (X = Cl, Br): A DFT Perspective," *International Journal of Multidisciplinary Research and Publications (IJMRAP)*, Volume 7, Issue 5, pp. 56-62, 2024.

KFeBr3 has its highest reflectivity peak at 14.6024eV while that of $KFeCl_3$ is at 16.31061eV. The reflectivity values are 0.3169 for $KFeBr_3$ and 0.5135 for $KFeCl_3$ at 0 eV. In terms of absorption, the main peak occurs at 13.1371eV for $KFeBr_3$ and at 14.1728eV for $KFeCl_3$. Both compounds show zero absorption at this energy level (0eV). For refractive index (n), the primary peak is situated at 1.690eV in the case of $KFeBr_3$ whereas it lies at 2.30012eV in the case of $KFeCl_3$. At this same energy value (0 eV), refractive index(n) values are equal to 2.3436 and to2.0584 for n. The real component of the dielectric function reaches its maximum value at an energy level equal to 8.970 eV in the case of compound AB while in compound BA it does so only when this same variable equal $13.00195eV$ mainly used as comparison points with other materials where they may appear close together or far apart from each other depending upon what was being compared against them. The real part increases monotonically towards infinity as frequency increases but oscillates continuously between negative values around zero until reaching one positive maximum before continuing towards negative infinite after which point another positive maximum is achieved prior to another negative infinite; imaginary components always remain zero throughout all frequencies considered herein such result not possible since would require one component be non-zero over some range where other is also nonzero simultaneously implying existence either absorption bands located between these two points or conductivity band overlapping with absorption bands situated below them. A similar situation was observed here too especially around the resettable range where loss function values become very significant at 23.4392eV for $KFeBr_3$ and at 16.9451eV for $KFeCl_3$; this implies that one of the materials is absorbing strongly while the other is not absorbing at all so these two could therefore have been obtained from different experiments or even different samples altogether [23].

IV. Conclusion

This is the first time we have performed a structural adjustment, band gap fine-tuning, and optical response analysis of halide perovskites $KFeBr_3$ and $KFeCl_3$ using first-principles calculations. All the calculations were done using CASTEP code which uses density functional theory, PBE-GGA exchange-correlation functional, and ultra-soft pseudopotentials. The results confirm that the computed values of band gaps and optimized lattice parameters for $KFeBr_3$ and $KFeCl_3$ are in agreement with those reported earlier. However, it should be noted that this work gives optimized structural data for these compounds for the first time. In addition to that, our calculated elastic constants fulfill mechanical stability conditions which imply that both materials are brittle according to Pugh's criterion. Further analysis shows that A factor indicates anisotropy in both materials. For $KFeBr_3$ VBM = CBM i.e. they coincide hence it has a direct band gap while in $KFeCl_3$ VBM ≠ CBM it's an indirect band gap. We also study various optical properties such as absorption, reflection, energy loss function, and refractive index in terms of their electronic features as well as the structures involved therein. According to our findings at 0 K, both substances exhibit insulating behavior whereas at higher temperatures they show semiconducting properties. Moreover, the dispersion imaginary part dielectric function suggests a wide energy transparency window which implies the possibility of capturing ultraviolet region optoelectronic device applications

References

[1] S. Tan *et al.*, "Temperature-reliable low-dimensional perovskites passivated black-phase CsPbI3 toward stable and efficient photovoltaics," *Angewandte Chemie International Edition*, vol. 61, no. 23, p. e202201300, 2022.
[2] Q. Ou *et al.*, "Band structure engineering in metal halide perovskite nanostructures for optoelectronic applications," *Nano Materials Science*, vol. 1, no. 4, pp. 268-287, 2019.
[3] S. J. Adjogri and E. L. Meyer, "A review on lead-free hybrid halide perovskites as light absorbers for photovoltaic applications based on their structural, optical, and morphological properties," *Molecules*, vol. 25, no. 21, p. 5039, 2020.
[4] M. Seri *et al.*, "Toward real setting applications of organic and perovskite solar cells: A comparative review," *Energy Technology*, vol. 9, no. 5, p. 2000901, 2021.
[5] S. H. S. S. Dintakurti, "Phase evolution and local structure in [Cs, MA][Pb, Sr][Cl, Br] 3 perovskites," 2021.
[6] E. F. C. Diaz and J. Calusdian, "Improving The Endurance Of Small Unmanned Aerial Vehicles Utilizing Flexible Solar Cells," 2022.
[7] P. Schulz, D. Cahen, and A. Kahn, "Halide perovskites: is it all about the interfaces?," *Chemical reviews*, vol. 119, no. 5, pp. 3349-3417, 2019.
[8] A. Belous, A. Ishchenko, O. V'yunov, and P. Torchyniuk, "Preparation and properties of films of organic-inorganic perovskites MAPbX3 (MA= CH3NH3; X= Cl, Br, I) for solar cells: a review," *Theoretical and Experimental Chemistry*, vol. 56, no. 6, pp. 359-386, 2021.
[9] M. A. Afroz *et al.*, "Design potential and future prospects of lead-free halide perovskites in photovoltaic devices," *Journal of Materials Chemistry A*, vol. 11, no. 25, pp. 13133-13173, 2023.
[10] Y. Zhao and K. Zhu, "Organic–inorganic hybrid lead halide perovskites for optoelectronic and electronic applications," *Chemical Society Reviews*, vol. 45, no. 3, pp. 655-689, 2016.
[11] M. Segall *et al.*, "First-principles simulation: ideas, illustrations and the CASTEP code," *Journal of physics: condensed matter*, vol. 14, no. 11, p. 2717, 2002.
[12] B. Saparov and D. B. Mitzi, "Organic–inorganic perovskites: structural versatility for functional materials design," *Chemical reviews*, vol. 116, no. 7, pp. 4558-4596, 2016.
[13] J. U. Rehman *et al.*, "A DFT study to investigate structural, electronic, optical, mechanical and magnetic properties of NaGeBr3 for photovoltaic and optoelectronic applications," *Emergent Materials*, vol. 6, no. 2, pp. 699-709, 2023.
[14] M. Akaogi, Y. Shirako, H. Kojitani, T. Nagakari, H. Yusa, and K. Yamaura, "High-pressure transitions in NaZnF3 and NaMnF3 perovskites, and crystal-chemical characteristics of perovskite–postperovskite transitions in ABX3 fluorides and oxides," *Physics of the Earth and Planetary Interiors*, vol. 228, pp. 160-169, 2014.
[15] M. Usman *et al.*, "First-principles calculations to investigate variation in the bandgap of NaSrF3 Fluoro-Perovskite with external static isotropic pressure and its Impact on optical properties," *Computational and Theoretical Chemistry*, vol. 1214, p. 113766, 2022.
[16] J. U. Rehman *et al.*, "A DFT study to investigate structural, electronic, optical, mechanical and magnetic properties of NaGeBr3 for photovoltaic and optoelectronic applications," *Emergent Materials*, vol. 6, no. 2, pp. 699-709, 2023.
[17] J. ur Rehman *et al.*, "First-principles calculations to investigate structural, electronic and optical properties of Na based fluoroperovskites NaXF3 (X= Sr, Zn)," *Solid State Communications*, vol. 334, p. 114396, 2021.
[18] H. Bouafia *et al.*, "Theoretical investigation of structural, elastic, electronic, and thermal properties of KCaF3, K0. 5Na0. 5CaF3 and

NaCaF3 Perovskites," *Superlattices and Microstructures*, vol. 82, pp. 525-537, 2015.
[19] G. Surucu, "Investigation of structural, electronic, anisotropic elastic, and lattice dynamical properties of MAX phases borides: An Ab-initio study on hypothetical M2AB (M= Ti, Zr, Hf; A= Al, Ga, In) compounds," *Materials Chemistry and Physics*, vol. 203, pp. 106-117, 2018.
[20] F. Birch, "Finite elastic strain of cubic crystals," *Physical review*, vol. 71, no. 11, p. 809, 1947.
[21 V. Sakhnenko and N. Ter-Oganessian, "Theory of order–disorder phase transitions of B-cations in AB′ 1/2B″ 1/2O3 perovskites," *Acta Crystallographica Section B: Structural Science, Crystal Engineering and Materials*, vol. 74, no. 3, pp. 264-273, 2018.
[22] R. Terki, H. Feraoun, G. Bertrand, and H. Aourag, "Full potential calculation of structural, elastic and electronic properties of BaZrO3 and SrZrO3," *Physica status solidi (b)*, vol. 242, no. 5, pp. 1054-1062, 2005.
[23] M. S. Alam, M. Saiduzzaman, A. Biswas, T. Ahmed, A. Sultana, and K. M. Hossain, "Tuning band gap and enhancing optical functions of AGeF3 (A= K, Rb) under pressure for improved optoelectronic applications," *Scientific Reports*, vol. 12, no. 1, p. 8663, 2022.

Ahmed Shahzad, Naseeb Ahmad, Muhammad Arbaz, Ifra Shahzadi, Moazama Ahsan, Zia Ur Rehman, Rizwan Akbar, Muhammad Kashif Bashir, Shahbaz Ali, “Exploring the Optoelectronic Potential of Cubic Halide-Perovskite KFeX3 (X = Cl, Br): A DFT Perspective,” *International Journal of Multidisciplinary Research and Publications (IJMRAP)*, Volume 7, Issue 5, pp. 56-62, 2024.